

INTERACTION OF LASER RADIATION WITH MATTER DOI: 10.1070/QEL16113

Simulation of spatial distribution of absorbed laser energy in spherical microcapsules

Yu.E. Geints, A.A. Zemlyanov, E.K. Panina

Abstract. **Specific features of optical field distribution in composite spherical particles consisting of a liquid core and nanocomposite absorbing shell are theoretically studied at different wavelengths of incident radiation. Using the numerical simulation it is shown that the thickness of the shell of the spherical microcapsule particle and its intrinsic absorption coefficient determine the character of the spatial distribution and the absorbed power. The variation of these parameters allows one to change the spatial position of efficient volume absorption regions and peak absorption values. This provides favourable conditions for opening the shells in appropriate spatial zones to release the contents of the microcapsules.**

Keywords: *spherical microcapsule, numerical electrodynamics method.*

1. Introduction

The progress in optical technology leads to miniaturisation of components of various optical devices and, therefore, to the necessity of making and using micro- and nanoscale optical diffraction elements. Such microobjects, in particular, spherical microparticles, are also of undoubted interest for different fields related to the development of chemical and biological technologies, cosmetology, and the development of optoelectronic devices [1–3]. The composite (multilayer) spherical particles are unique from the point of view of using them as miniature portable systems, active biological labels based on plasmonic nanolasers (spasers) [4, 5], as well as containers for capsulation of various substances [6, 7].

Multiple studies have shown that spherical microcapsules possess great potentialities as delivery containers. Their properties depend on the thickness and optical properties of the shell, and the functional capabilities are dictated by the destination of the contained substance. One of the achievements of modern physics and chemistry is the technology of producing micro- and nanocapsules with nanoscale shells [8–10], which can be controllably opened under the action of a number of factors (temperature, laser radiation, acidity of the medium). The technology of making the capsules based on polyelectrolytes was developed in Ref. [11]. Using the so-called polyionic assembly method [12, 13], in which by sequential adsorption of polymers or nanoparticles the surface of a particle containing the required substance is coated with a polymer or nanocomposite shell [14]. The shell protects the contents of the microcapsule, but it is sensitive to electromagnetic radiation. In Ref. [15] the results of experimental studies of the microwave radiation effect on polymer microcapsules are presented. Using the results of scanning electron microscopy of the capsules, it was found that the effect of radiation depends on the microcapsule composition, the frequency and the power of incident radiation.

At present, there are several strategically important applications of microcapsules. In medicine it is proposed to use microcapsules as systems of addressed delivery of biologically active components to cells and tissues [16–18]. In future, this will allow one to reduce doses of medicinal preparations by several times and to eliminate side effects. The main problem here is not only the delivery of a microcapsule to the appropriate organ, but also its timely opening. The drug released from the capsule affects target cells without damaging adjacent tissues.

The approaches are also developed to transporting in microcapsules the nanostructures of metallic and semiconductor nature for selective destruction of cells under electromagnetic heating, which is important for the treatment of some tumours [19]. Thus, it is important not only to create miniature capsules with prescribed properties, but also to control their travelling and opening remotely, e.g., using electromagnetic radiation. The solution of these problems will essentially extend the possibilities of using composite spherical particles in medicine, nano- and microelectronics, as well as in chemical industry.

The studies of the possibility of opening microcapsules have already been carried out. Thus, the authors of Refs [20, 21] showed that one of the methods for destroying polyelectrolyte shells could be based on the remote action of laser radiation on the capsules, modified by nanoparticles of metal. However, the results of these studies do not allow one to predict how the opening process of microcapsules will change in the case of changing their dimensions, absorption and radiation wavelength. The additional theoretical studies are required here, including the investigation of the optical field redistribution in a microcapsule under the variation of its parameters.

In the present paper, we report the results of theoretical studies of the optical field distribution inside composite spherical particles consisting of a liquid core and a polymer absorbing shell, exposed to laser radiation. These particles are an analogue of microcapsules used in medicine. Using the finite difference time domain (FDTD) method of computational electrodynamics, we simulate the spatial structure of the light wave absorbed power in double-layer spherical par-

Yu.E. Geints, A.A. Zemlyanov, E.K. Panina V.E. Zuev Institute of Atmospheric Optics, Siberian Branch, Russian Academy of Sciences, pl. Akad. Zueva 1, 634055 Tomsk, Russia; e-mail: ygeints@iao.ru

Received 25 April 2016; revision received 11 July 2016
Kvantovaya Elektronika **46** (9) 815–820 (2016)
Translated by V.L. Derbov

ticles under the variation of the radiation wavelength, shell thickness and optical properties. We show that the variation of the absorption in the shell of a composite particle allows the structure modification of the inner optical layer, in particular, the essential enlargement of 'hot zones', corresponding to the regions of maximal absorbed power. This extends the possibilities of choosing the optimal conditions for perforating the shells of the microcapsules in the implementation of particular practical applications.

2. Method and results of theoretical modelling

In the calculations, we used the widespread method of numerical solution of the electrodynamic problems, based on the direct solution of the system of Maxwell differential equations by means of approximating the differential operators with finite difference schemes in the spatiotemporal domain. The use of this FDTD method dates from the early work by K.S. Yee [22] and A. Taflove [23], where the approach to the application of finite-difference computational schemes to a system of vortex partial differential equations of the first order, to which the Maxwell equations belong, was formulated and developed. The base element of these schemes, both implicit and explicit, is the so-called Yee cell, in which all projections of the electromagnetic field vectors onto the Cartesian axes are spatially arranged in a special way. The components of the electric vector E are localised at the middle of the edges, while the components of the magnetic vector H are localised at the centres of faces. All components enter Maxwell's equations; besides that, the fields E and H are calculated with the time shift by a half of the time step. The implementation of such a stepwise grid allows the achievement of the second-order spatiotemporal accuracy in the solution of Maxwell's equations.

The algorithm of the field calculation is an evolutional one, i.e., the mesh values of the functions in the current time layer are calculated using the values found at the previous layer. To prevent the reflection from the boundaries, all computation space, as a rule, is enclosed in a matrix containing a set of perfectly matched layers (PML) that possess a low reflection coefficient even for acute angles of wave incidence, although the presence of such a layered structure considerably increases the requirements to computing resources. The outer boundaries of the computation domain consist of a perfectly absorbing layer. All numerical calculations, the results of which are presented below, are carried out using the programme package elaborated by the authors. The kernel of this package is the open-code programme module 3D FDTD-X2 written in C++ [24] and modified for particular computing configurations.

The considered model was a spherical particle, consisting of a unabsorbing liquid core having the radius R_c and the refractive index $n_c = 1.33$ (water) and an optically denser radiation-absorbing shell having the thickness a_s. The real part n_s of the complex refractive index $m_s = n_s - i\kappa_s$ of the shell was equal to 1.5. This value lies within the range of typical values for real polymers constituting a nanocapsule shell ($n_s = 1.48-1.52$ [25, 26]). The medium, surrounding the double-layered particle, is also considered to be water, $n_0 = n_c$.

In the calculations the absorption index of the particle shell κ_s was varied within the range 0.001–1. Under real conditions, such a variation of κ_s is possible due to the introduction of nanoparticles (metal, dielectric) into the dense polymer shell to enhance the radiation absorption in the required wavelength range.

Indeed, according to the Maxwell Garnett effective medium theory [27] we have for a two-component mixture

$$\varepsilon_s = m_s^2 = \varepsilon_{lat}\frac{\varepsilon_p(1+2\delta)+2\varepsilon_{lat}(1-\delta)}{\varepsilon_p(1-\delta)+\varepsilon_{lat}(2+\delta)}, \quad (1)$$

where δ is the volume fraction of the solid-state absorbing component (sol); and $\varepsilon_p = \varepsilon_p' - i\varepsilon_p''$ and ε_{lat} are the permittivities of the sol and the basic substance considered unabsorbing. It is known [28] that the Maxwell Garnett model sufficiently well describes the dielectric properties of a composite medium, when the volume fraction of one component is much smaller than that of the other, i.e., when $\delta \ll 1$ or $1-\delta \ll 1$. This situation is usually observed when a small fraction of strongly absorbing nanoparticles is added to the transparent matrix. Note that for a more precise description of the multicomponent medium one can use, e.g., the Bruggeman model [29, 30].

If the sol particles are metallic nanospheres, then for the determination of ε_p one can use the optical model of a solid metal (the Drude model), corrected to allow for the effect of the geometric dimension of the particle on the collision rate of free electrons [31] (only the dipole plasmon resonance is assumed to be excited)

$$\varepsilon_p = \varepsilon_{pb}(\omega) + 1 - \frac{\omega_p^2}{\omega^2+\omega_c^2}\left(1+i\frac{\omega_c}{\omega}\right), \quad \omega_c = v_F\left(\frac{1}{l_e}+\frac{1}{a_0}\right). \quad (2)$$

Here ε_{pb} is the permittivity of the solid metal; ω is the circular frequency of radiation; ω_p is the plasma frequency; v_F is the Fermi velocity; l_e is the mean free path length of the electron; and a_0 is the sol particle radius.

For example, Fig. 1 presents the spectral dependence of the volume absorption coefficient $\alpha_s = 4\pi\kappa_s/\lambda$ (λ being the radiation wavelength) of the composite polymer with the addition of silver spherical nanoparticles calculated using formulae (1) and (2). For the calculations we used the following parameters of the solid silver: $\omega_p = 13.4$PHz, $v_F = 1.38 \times 10^6$ m s^{-1}, $l_e = 57$ nm, and the dependence $\varepsilon_{pb}(\omega)$ was adopted from Ref. [32].

In the figure, one can see a characteristic absorption peak of the metallic composite, caused by the excitation of the fun-

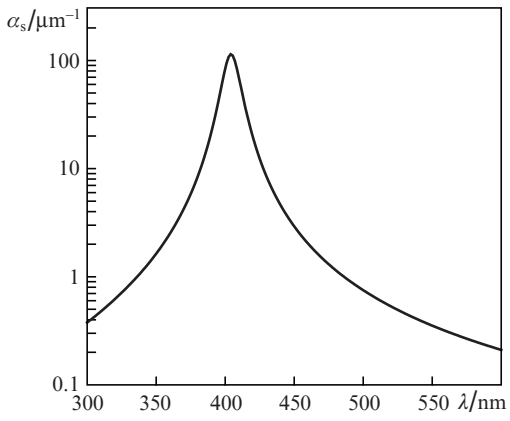

Figure 1. Absorption spectrum of spherical silver nanoparticles with the volume fraction $\delta = 10^{-4}$ and the radius $a_0 = 10$ nm in polymer matrix ($\varepsilon_{lat} = 2.25$-i•0).

damental (Fröhlich mode) surface plasmon resonance of the silver sphere at $\lambda \sim 410$ nm. Increasing the size of sol particles leads to the reduction of the effective rate of electron collisions in the metal and, therefore, to a decrease in light absorption in the entire spectral range. Besides that in the spectrum of collective surface oscillations of electrons in metallic nanoparticles, the multipole effects become noticeable, leading to a spectral shift of the plasmon resonance and a change in its shape [33]. The use of other metal particles (gold, aluminium, etc.) as the component absorbing optical radiation shifts the absorption maximum of the polymer composite of the microcapsule shell to the other spectral region due to the analogous shift of the plasmon resonance [34]. This effect allows selective opening of a microcapsule by adding different metals to the shell and varying the exposure wavelength.

To determine the spatial profile of the radiation power P_{ab} absorbed in the microcapsule, the model particle was placed in a cubic volume with linear dimensions $3 \times 3 \times 3$ μm, in which the spatial mesh containing $\sim 10^6$ nodes was introduced. At the lower face of the computation domain a plane linearly polarised wave was specified with the wavelength λ (circular frequency ω) and the amplitude $E_0 = 1$ V m^{-1} to be further diffracted by the particle. After the time averaging of the optical fields calculated using the FDTD algorithm over the time interval ~ 1 ps, we calculated the spatial distribution of the absorbed power

$$P_{ab} = \frac{\varepsilon_0}{2} \varepsilon'' \omega_0 |\boldsymbol{E}|^2,$$

where ε'' is the imaginary part of the complex permittivity of the medium, ε_0 is the permittivity of vacuum; $\omega = 2\pi c/\lambda$; and c is the velocity of light in vacuum.

For convenience of interpreting the results, we analyse not the locally absorbed power itself, but the effective absorption coefficient α_{ab}, defined by normalising the power P_{ab} to the intensity of the incident optical wave $I_0 = (cn_0/2)\varepsilon_0 |E_0|^2$

$$\alpha_{ab}(\boldsymbol{r}) = \frac{P_{ab}}{I_0} = \frac{2\pi\varepsilon''}{\lambda n_0} B(\boldsymbol{r}), \qquad (3)$$

where $\boldsymbol{r}$ is the radius-vector of a point inside the particle; $B = |\boldsymbol{E}|^2/E_0^2$ is the factor of inhomogeneity of the intensity distribution of the optical field. Obviously, the greater the α_{ab}, the stronger the absorption of radiation in the given spatial point.

The distributions of the coefficient α_{ab} over the longitudinal equatorial section of the spherical capsule under the variation of the absorption index κ_s and the thickness a_s of the shell is demonstrated by a series of images in Fig. 2. In the calculations, the outer radius of the particle $R_0 = R_c + a_s$ was fixed and equal to 1 μm. The incident light wavelength was 0.532 μm. The figures in the images are the maximal values of α_{ab} within the section shown.

The qualitative comparison of the obtained spatial distributions reveals their essential difference depending on the ratio of the core and the shell geometric size, as well as on the level of the shell intrinsic absorption. As known from Mie theory [35], in the course of diffraction of a plane electromagnetic wave on a double-layer particle, the regions of increased intensity ('hot zones') are formed along the optical axis of the particle, which, as a rule, are located near the surface in the illuminated and shadow hemispheres of the particle. The magnitude of the peak intensity and the dimensions of these 'hot zones' depend on the structure of the double-layer particle.

The increased absorption in the shell of a composite particle leads to redistribution of its optical field. In the case of a thin and weakly absorbing shell (Fig. 2a), a localised zone of increased α_{ab} values appears at the shadow surface of the microcapsule. However, the spatial dimensions of this region are very small, and the absorption is weak, which does not allow this microparticle configuration to be considered efficient for destroying the capsule shell.

The most advantageous in this sense is the case presented in Fig. 2d, corresponding to $\kappa_s = 0.01$. It is seen that in this case the region of absorbed power is uniformly distributed over the entire volume of the microcapsule shell. A further increase in κ_s leads to the shift of the α_{ab} maximum to the lower hemisphere of the particle (Fig. 2g). The spatial dimensions of this region amount to nearly half a particle, and the effective volume absorption coefficient of the particle α_{ab} in the maximum is by two orders of magnitude greater than in Fig. 2a.

The corresponding radial distributions of the absorbed power of radiation along the principal cross section of double-layer microparticles with the fixed shell thickness $a_s = 0.3$ μm are presented in Fig. 3. As in the previous study, the absorption index κ_s of the shell was varied within a wide range. The longitudinal coordinate is relative to the shadow surface of the microcapsule. It is seen how the character of the field distribution changes with the growth of κ_s. While for a weakly absorbing shell (Fig. 3a) the field maximum is located near the shadow surface of the particle, for $\kappa_s = 0.1$ one can clearly see two expressed peaks near the shadow and illuminated surfaces (Fig. 3b). A further increase in κ_s in the particle shell is accompanied by the shift of the region where the peak values of α_{ab} take place to the illuminated hemisphere and by the narrowing of this zone. For high values of κ_s the region of maximal α_{ab} becomes localised in the near-surface layer (Fig. 3c), which can be a matter of principle from the point of view of destructing the microcapsule shell without affecting its contents.

The results of numerical calculations, illustrating the effect of the shell thicknessa_s of the model spherical microcapsule on its effective volume absorption coefficient α_{ab}, are presented in Fig. 4. It follows from the figure that this dependence exists only for the moderate and weak absorption of the particle shell ($\kappa_s < 1$). One can see that for such situations the dependences $\alpha_{ab}(a_s)$ exhibit an extremum [curves (*1*, *2*)] for $a_s \sim 200$ nm, which is explained by the specific character of the formation of the shell internal field structure.

Indeed, as mentioned above, the regions of increased intensity of the internal field are formed near the shadow and illuminated surface of the particle as a result of the constructive interference of the transmitted and diffracted waves. In fact, these regions are zones of internal foci of geometric optical rays, once refracted by the particle and reflected from its internal surface. In a hollow shell sphere, the fraction of rays gathered near the internal focus is proportional to the thickness of the contrast shell. Hence, in the case of a weakly absorbing shell the decrease in its thickness leads to the fall of the intensity B (and, therefore, the absorbed power) in the foci, and vice versa. This trend can be traced in the left-hand part of the discussed curves.

On the other hand, the presence of absorption in the shell material negatively affects, first, the intensity of refracted and reflected waves, forming the back (shadow) focus. In this

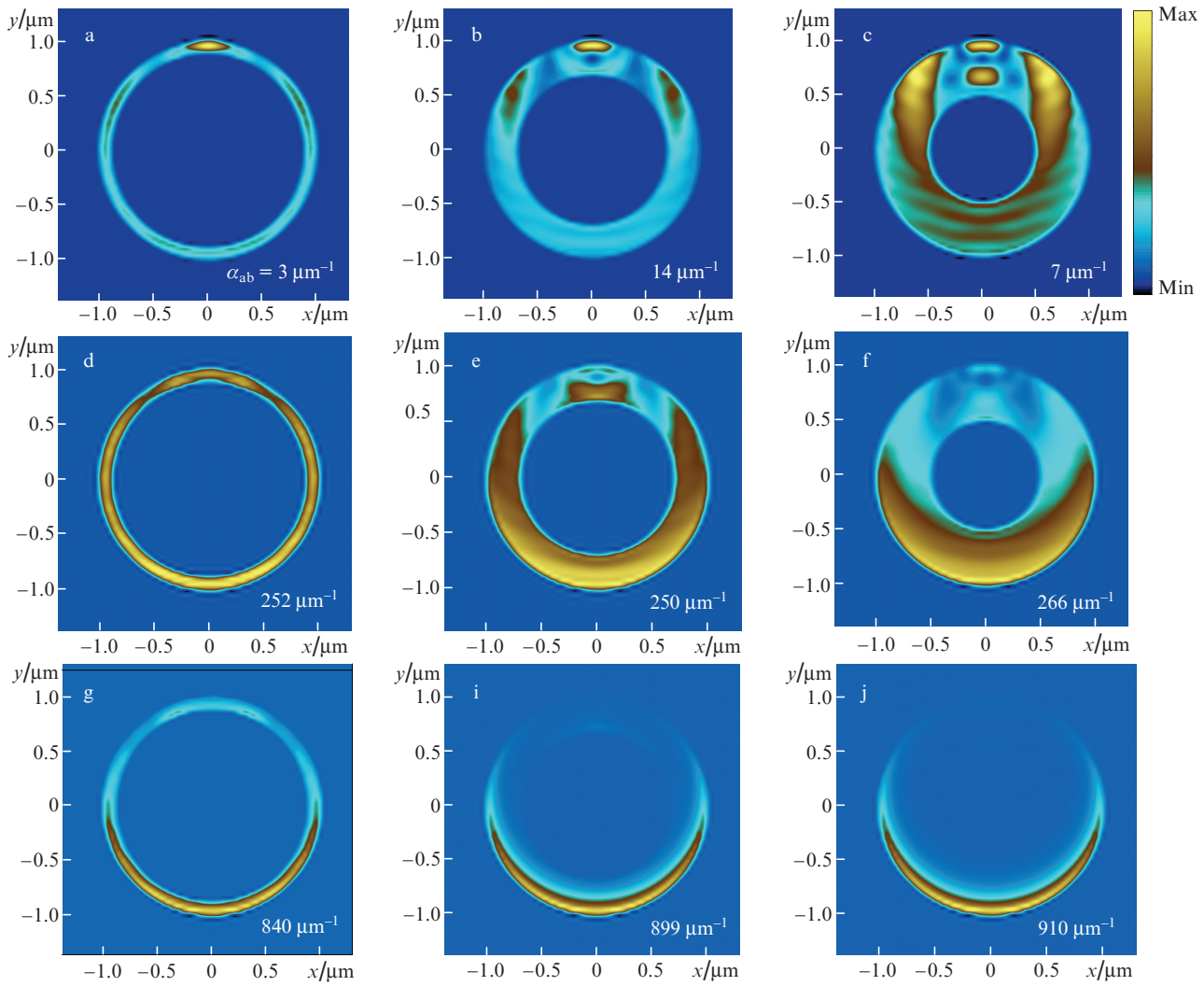

Figure 2. Profiles of the effective coefficient of volume absorption α_{ab} inside the composite double-layer particles having the radius $R_0 = 1$ μm and the shell thickness a_s = (a, d, g) 0.1, (b, e, h) 0.3, and (c, f, i) 0.5; the absorption index κ_s = (a–c) 0.001, (d–f) 0.1, (g–i) 0.5. The incident radiation wavelength is $\lambda = 0.532$ μm. The radiation is incident from below.

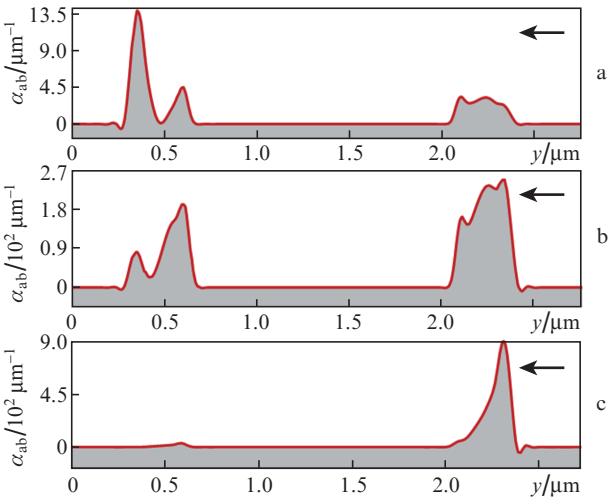

Figure 3. Radial distributions of α_{ab} along the principal cross section of composite spherical particles having the radius $R_0 = 1$ μm and the shell thickness $a_s = 0.3$ μm; the absorption index of the shell κ_s = (a) 0.001, (b) 0.1 and (c) 0.5, the incident radiation wavelength is $\lambda = 0.532$ μm. The arrow shows the direction of incidence.

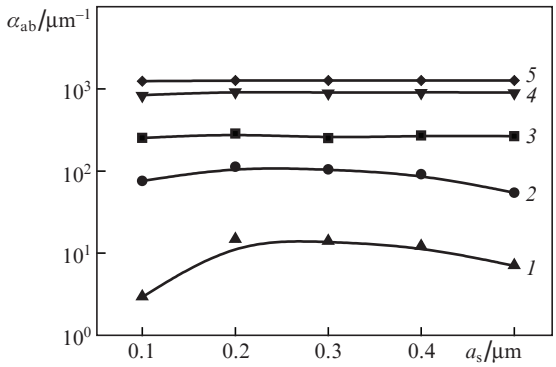

Figure 4. Dependences of the maximal values of the effective volume absorption coefficient of microcapsules α_{ab} ($R_0 = 1$ μm) on the shell thickness a_s for κ_s = (*1*) 0.001, (*2*) 0.01, (*3*) 0.1, (*4*) 0.5 and (*5*) 1. The incident radiation wavelength $\lambda = 0532$ μm.

case, the relative fraction increases for the 'direct' radiation, propagating along the particle diameter and making small angles with the optical axis, so that the optical path inside the sphere is minimal. The thicker the microcapsule shell, the

weaker the light rays, refracted by it. This reduces the lensing effect of the spherical particle and leads to a decrease in the internal field intensity, due to which the profile of the absorption coefficient distribution becomes sickle-shaped (see Figs 2g–2i). The discussed extremum of the peak α_{ab} values is just a result of the competition of these two processes.

At high values of the absorption index of the microcapsule shell material κ_s [curves (*3–5*) in Fig. 4] the maximum of the particle absorption coefficient α_{ab} weakly depends on the shell thickness a_s, and the incident radiation is completely absorbed in the illuminated part of the particle. Hence, in this case, the achievement of the maximal heat release already does not require a precise control of the shell thickness, and one can choose the value of a_s, based on the real technological possibilities of coating microobjects with thin shells having a variable absorption index.

The variation of the optical field distribution of the shells of spherical microcapsules is also possible by changing the wavelength of radiation acting on the particles of fixed radius. Figure 5 presents 2D distributions of the absorbed power inside the shelled spherical particles differing by the shell thickness. Similar to Fig. 2, the figures correspond to the maximal α_{ab} values. The absorption index of the shell was $\kappa_s = 0.001$, the wavelength of the incident radiation varied from 0.245 to 0.8 μm.

The comparison of Figs 5a–5f shows that with the transition to both shorter and longer wavelengths of the incident radiation the configuration of the absorbed power region in the microcapsule shell also changes. First, the shortening of the radiation wavelength leads to a significant increase in the absorption coefficient of the composite particles. Second, the configuration of the absorption zone in the shell is drastically changed. It is seen that under the exposure of the particle to the radiation, e.g., in the near-infrared spectral region (Figs 5e and 5f) the absorption zone, compared to the case of visible light exposure, occupies practically the entire volume of the shell, although the maximal values of the effective volume absorption coefficient α_{ab} are not high.

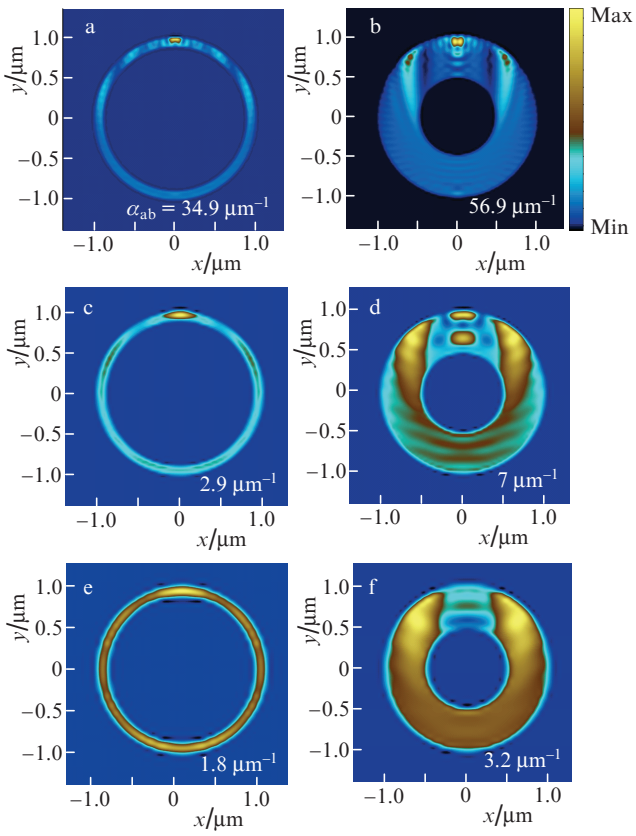

Figure 5. Distributions of the effective coefficient of the radiation absorption in the shells of the composite particles having the radius R_0 = 1 μm, exposed to the radiation with λ = (a, b) 0.245, (c, d) 0.532 and (e, f) 0.8 μm. The absorption index is $\kappa_s = 0.001$, the shell thickness is a_s = (a, c, e) 0.1 and (b, d, f) 0.5 μm. The radiation is incident from below.

Besides that, in the case of UV radiation (Figs 5a and 5b) the growth of the microcapsule shell thickness does not lead to essential changes in the spatial position of the absorption maximum, as in the case of the visible and IR radiation, but multiply increases α_{ab}. Here one can clearly see the highly localised point zone of the maximal values of energy dissipation, always located near the shadow surface of the capsule, the small size of which can inhibit the destruction of the entire shell of the microparticle.

On the contrary, in the case of exposing the microcapsules to the radiation with $\lambda = 0.532$ μm, the greater thickness of the particle shell (Fig. 5d) leads to the formation of a few clearly expressed peaks of absorption α_{ab} in the shadow hemisphere, rather than a single peak. The spatial dimensions of the zone of maximal values of the absorbed power increase, and the structure of the optical field in the shell becomes more complicated.

In the field of long-wavelength radiation (Figs 5e and 5f) with an increase in the shell thickness a_s the configuration of the α_{ab} distribution also changes. While for a capsule with thin walls (Fig. 5e) the absorbed power demonstrates a practically uniform distribution over the entire volume of the shell, in a thick-wall capsule (Fig. 5f) the maximum of absorption is shifted towards the illuminated (bottom) surface of the particle and occupies the most part of the shell, negatively affecting the absorption coefficient amplitude.

3. Conclusions

Thus, we have considered the specific features of the optical field formation in the composite double-layer spherical particles (microcapsules), having the outer radius 1 μm, exposed to optical radiation. It is shown that the main factors affecting the character of the spatial distribution and the amplitude characteristics of the absorbed power inside the microcapsule shell are the shell thickness and the value of the coefficient of its intrinsic radiation absorption. The numerical simulation carried out using the method of computational electrodynamics clearly demonstrated that by increasing the absorption in the shell one can significantly increase the extension of the region of efficient volume absorption of the particle and make its peak values higher by a few orders of magnitude. The change in the shell thickness leads to the redistribution of the absorbed power inside the microcapsule, and the thick-wall microcapsules absorb radiation predominantly by their illuminated hemisphere. Moreover, we have found the possibility of modifying the characteristics of the absorption regions in the shells of spherical microcapsules of fixed radius by varying the wavelength of incident radiation. This allows controllable creation of optimal conditions for opening the shells at the required spatial zones with the purpose to release the contents of the microcapsules.

Acknowledgements. The authors thank reviewers for critical remarks that made it possible to essentially improve the present paper.

References

1. Feldheim D.L., Keating C.D. *Chem. Soc. Rev*., **28**, 1 (1998).
2. Dabbousi B.O., Bawendi M.G., Onitsuka O., Rubner M.F. *Appl. Phys. Lett*., **66** (11), 1316 (1995).
3. Colvin V.L., Schlamp M.C., Alivisatos A.P. *Nature*, **370**, 354 (1994).
4. Bergman D.J., Stockman M.I. *Phys. Rev. Lett.*, **90**, 027402 (2003).
5. Galanzha E.I., Weingold R., Nedosekin D.A., Sarimollaoglu M., Kuchyanov A.S., Parkhomenko R.G., Plekhanov A.I., Stockman M.I., Zharov V.P. https://arhiv.org/ftp/arhiv/papers/1501/1501.00342.pdf.
6. Bukreeva T.V., Feigin L.A. *Priroda*, **12**, 78 (2013).
7. Bukreeva T.V., Marchenko I.V., Borodina T.N., et al. *Dokl. Akad. Nauk*, **440** (2), 191 (2011) [*Dokl. Phys. Chem*., **440** (1), 165 (2011)].
8. Antipov A.A., Shchukin D., Fedutik Y., Petrov A.I., Sukhorukov G.B., Mohwald H. *Colloid. Surf. Physicochem. Eng. Aspects*, **224**, 175 (2003).
9. Cheng D., Xia H., Chan H.S.O. *Nanotechnol.*, **17** (6), 1661 (2006).
10. Sukhorukov G.B., Donath E., Davis S., Lichtenfeld H., Caruso F., Popov V.I., Mohwald H. *Polym. Adv. Technol*., **9** (10-11), 759 (1998).
11. Donath E., Sukhorukov G.B., Caruso F., Davis S.A., Mohwald H. *Angew. Chem. Int. Ed*., **37** (16), 2202 (1998).
12. Iler R.K. *J. Coll. Int. Sci*., **21** (6), 569 (1966).
13. Decher G., Hong J.D. *Macromol. Chem. Sym*., **46**, 321 (1991).
14. Sukhorukov G.B., Donath E., Davis S., Lichtenfeld H., Caruso F., Popov V.I., Möhwald H. *Polym. Adv. Technol*., **9**, 759 (1998).
15. Gorin D.A., Shchukin D.G., Mikhailov A.I., Köhler K., Sergeev S.A., Portnov S.A., Taranov I.V., Kislov V.V., Sukhorukov G.B. *Pis'ma Zh. Tekh. Fiz*., **32**, 45 (2006) [*Tech. Phys. Lett*., **32** (1), 70 (2006)].
16. De Koker S., Lambrecht B.N., Willart M.A., van Kooyk Y., Grooten J., Vervaet C., Remon J.P., De Geest B.G. *Chem. Soc. Rev*., **40** (1), 320 (2011).
17. Cock L.J., De Koker S., Geest B.G., Grooten J., Vervaet C., Remon J.P., Sukhorukov G.B., Antipina M.N. *Angewandte Chem. Intern. Ed*., **49**, 6954 (2010).
18. Borodina T.N., Rumsh L.D., Kunizhev S.M., Sukhorukov G.B., Vorozhtsov G.N., Feldman B.M., Markvicheva E.A. *Biomed. Khim*., **53** (5), 557 (2007).
19. Avetisyan Yu.A., Yakunin A.N., Tuchin V.V. *Ross. Bioterapevt. Zh*., **4**, 89 (2011).
20. Bukreeva T.V., Parakhonsky B.V., Sukhorukov G.B., Skirtach A.G., Susha A.S. *Kristallografiya*, **51** (5), 183 (2006) [*Crystallogr. Rep*., **51** (5), 863 (2006)].
21. Skirtach A.G., Dejugnat C., Braun D., Susha A.S., Rogach A.L., Parak W.J., Möhwald H., Sukhorukov G.B. *Nano Lett*., **5**, 1371 (2005).
22. Yee K.S. *IEEE Trans. Antennas Propag*., **AP-14**, 302 (1966).
23. Taflove A., Hagness S. *Computational Electrodynamics: The Finite-Difference Time-Domain Method* (Boston: Arthech House Publ., 2000) p. 852.
24. http://www.its.caltech.edu/~seheon/FDTD.html.
25. Gorin D.A., Yashchenok A.M., Koksharov Yu.A., Neveshkin A.A., Serdobintsev A.A., Grigoriev D.O., Khomutov G.B. *Techn. Phys*., **54** (11), 1675 (2009).
26. Ruths J., Essler F., Decher G., Riegler H. *Langmuir*, **16**, 8871 (2000).
27. Born M., Wolf E. *Principles of Optics* (Oxford: Pergamon Press, 1970).
28. Golovan L.A., Timoshenko V.Yu., Kashkarov P.K. *Usp. Fiz. Nauk*, **177**, 619 (2007) [*Phys. Usp*., **177**, 595 (2007)].
29. Bruggeman D.A.G. *Ann. Phys. (Leipzig)*, **24**, 636 (1935).
30. Grigoriev D., Gorin D., Sukhorukov G.B., Yashchenok A., Maltseva E., Möhwald H. *Langmuir*, **23**, 12388 (2007).
31. Mandal S.K., Roy R.K., Pal A.K. *J. Phys. D: Appl. Phys*., **35** (17), 2198 (2002).
32. Palik E.D. (Ed.) *Handbook of Optical Constants of Solids. Vol. II* (San Diego: Elsevier Sci., 1998) p. 1096.
33. Klimov V.V. *Nanoplasmonics* (Singapore: Pan Stanford Publishing, 2014; Moscow: Fizmatlit, 2009).
34. Geints Y.E., Zemlyanov A.A., Panina E.K. *Izv. Vyssh. Uchebn. Zaved., Ser. Fiz*., **50** (4), 76 (2010) [*Russ. Phys. J*., **53** (4), 410 (2010)].
35. Bohren C.F., Hoffman D.R. *Absorption and Scattering of Light by Small Particles* (New York : Wiley, 1998).